

Towards an optimal search strategy of optical and gravitational wave emissions from binary neutron star coalescence

D. M. Coward,^{1*} B. Gendre,² P. J. Sutton,³ E. J. Howell,¹ T. Regimbau,⁴
M. Laas-Bourez,¹ A. Klotz,⁵ M. Boër⁶ and M. Branchesi^{7,8}

¹*School of Physics, University of Western Australia, Crawley WA 6009, Australia*

²*ASI Science Data Center, via Galileo Galilei, 00044 Frascati (RM), Italy*

³*School of Physics and Astronomy, Cardiff University, The Parade, Cardiff CF24 3AA*

⁴*Dpt. ARTEMIS, Observatoire de la Côte d'Azur, BP 429 06304 Nice, France*

⁵*Centre d'étude spatiale des rayonnements, Observatoire Midi-Pyrénées, CNRS, Université de Toulouse, BP 44346, F-31028 Toulouse Cedex 4, France*

⁶*Observatoire de Haute-Provence, F-04870 Saint Michel l'Observatoire, France*

⁷*DiSBeF - Università degli Studi di Urbino 'Carlo Bo', I-61029 Urbino, Italy*

⁸*INFN, Sezione di Firenze, I-50019 Sesto Fiorentino, Italy*

Accepted 2011 April 22. Received 2011 April 20; in original form 2011 February 20

ABSTRACT

Observations of an optical source coincident with gravitational wave emission detected from a binary neutron star coalescence will improve the confidence of detection, provide host galaxy localization and test models for the progenitors of short gamma-ray bursts. We employ optical observations of three short gamma-ray bursts, 050724, 050709 and 051221, to estimate the detection rate of a coordinated optical and gravitational wave search of neutron star mergers. Model *R*-band optical afterglow light curves of these bursts that include a jet-break are extrapolated for these sources at the sensitivity horizon of an Advanced LIGO/Virgo network. Using optical sensitivity limits of three telescopes, namely TAROT ($m = 18$), Zadko ($m = 21$) and an 8–10 m class telescope ($m = 26$), we approximate detection rates and cadence times for imaging. We find a median coincident detection rate of 4 yr^{-1} for the three bursts. GRB 050724 like bursts, with wide opening jet angles, offer the most optimistic rate of 13 coincident detections per year, and would be detectable by Zadko up to 5 d after the trigger. Late-time imaging to $m = 26$ could detect off-axis afterglows for GRB 051221 like bursts several months after the trigger. For a broad distribution of beaming angles, the optimal strategy for identifying the optical emissions triggered by gravitational wave detectors is rapid response searches with robotic telescopes followed by deeper imaging at later times if an afterglow is not detected within several days of the trigger.

Key words: gravitational waves – techniques: miscellaneous – gamma-ray burst: individual – stars: neutron.

1 INTRODUCTION

A multimessenger approach to gravitational wave (GW) detection is one of the most prioritized goals for second-generation ground-based gravitational wave detectors, such as Advanced LIGO (Harry et al. 2010) and Advanced Virgo (Acernese et al. 2009). It allows GW candidates that are too weak to claim detection based on GW data alone to be associated with an optical signal that could provide strong confirmation. Kochanek & Piran (1993) showed that in principle a joint electromagnetic–gravitational wave (EM–GW) search reduces the GW amplitude detection threshold by a factor of about 1.5. This has the effect of extending the sensitivity horizon distance of GW detectors for a binary neutron star merger (NS–NS), so that

the number of potentially detectable GW sources increases by a factor of ~ 3.4 . The benefits of joint EM–GW searches are significant on many fronts. For example, direct measurement of GWs from an NS–NS late inspiral and merger provides a means to determine luminosity distance; by combining GW-derived luminosity distance measurements with EM redshifts, one can constrain key cosmological parameters. Joint observations offer unprecedented insight into the complex astrophysics that are key to the EM emissions, offering the most complete picture from the strong to weak gravity regime.

One expected EM counterpart of an NS–NS merger is a short gamma-ray burst (SGRB), where ‘short’ is defined as $T_{90} < 2 \text{ s}$.¹

*E-mail: coward@physics.uwa.edu.au

¹ The duration in which the cumulative counts increase from 5 to 95 per cent above background.

The popular model for SGRBs is a compact object merger triggering an explosion causing a burst of collimated gamma-rays (Eichler et al. 1989; Narayan, Paczynski & Piran 1992; Lee, Ramirez-Ruiz & Granot 2005) powered by accretion on to the newly formed compact object. SGRBs are believed to be produced by dissipation of kinetic energy of ultrarelativistic outflow from the central engine with a Lorentz factor of $\Gamma \sim 100\text{--}1000$. The outflow is eventually decelerated by interaction with interstellar matter to produce a fading X-ray and optical afterglow. After Γ decreases to $\Gamma \sim \theta_j^{-1}$, where θ_j is the jet opening half-angle, the radiation beam is wider than the outflow, so the afterglow becomes observable from angles greater than θ_j .

Although NS–NS mergers are the favoured progenitor for SGRBs, other scenarios cannot be excluded, i.e. NS–BH mergers (McWilliams & Levin 2011) or magnetar outbursts (Nakar 2007). The main evidence is based on the association of some SGRBs with an older stellar population, as compared to ‘long’ GRBs, which are associated with massive stellar collapse. Evidence for the origin of SGRBs in the final merger stage comes from both the host galaxy types (e.g. Zheng & Ramirez-Ruiz 2007) and the measured offsets of GRBs from their host galaxies (e.g. Belczynski et al. 2006). Kicks imparted to NSs at birth will produce velocities of several hundred km s^{-1} , implying that binary inspiraling systems may occur far from their site of origin. Fong, Berger & Fox (2010), using *Hubble Space Telescope* observations to measure SGRB galaxy offsets, find that the offset distribution compares favourably with the predicted distribution for NS–NS binaries. However, they do not rule out at least a partial contribution from other progenitors systems.

1.1 GW-triggered SGRB afterglow search

A number of laser interferometric GW detectors have now reached their design sensitivities and have been operating as a global array, coordinating with EM observations through triggered follow-ups. These include the LIGO² detectors based at Hanford and Livingston in USA, the Virgo³ detector in Italy and the GEO 600⁴ detector in Germany. The LIGO and Virgo detectors are undergoing a series of upgrades towards advanced configurations that will produce an order of magnitude improvement in sensitivity. Advanced LIGO⁵ and Advanced Virgo⁶ are expected to be operational by 2015.

Because the coalescing binary NSs are expected to radiate GWs in the sensitivity band of Advanced LIGO/Virgo, coincident GW–EM observations of SGRBs will determine if the engine is an NS–NS or NS–BH binary merger. Furthermore, the rates of EM and coincident GW detections could constrain the distribution of jet collimation angles of SGRBs, crucial for understanding energetics (Berger et al. 2007). This is possible because the binary inclination angle to the line of sight is a GW observable.⁷ A direct consequence of collimation is that the rate of (both long and short) GRB afterglows should be higher than those observed as prompt bursts. SGRB afterglows observed ‘off-axis’ without a prompt counterpart have been termed ‘orphan afterglows’. There has not been a definitive discovery of an orphan afterglow, despite both dedicated searches to $m = 23$

and using archived data (Totani & Panaitescu 2002; Rau, Greiner & Schwarz 2006). The non-detection could partly be attributed to the small flux of off-axis afterglows, compared to on-axis ones that can be observed as early as seconds after the prompt burst and in some cases while the high-energy prompt emission is still occurring (Klotz et al. 2009).

The prospects might seem bleak for detecting off-axis afterglows. This is the case for an all-sky search, but a GW observation of an NS–NS inspiral collapses the search area from all-sky to the error ellipse (angular sky resolution) of the GW detectors. For such events, the angular resolution of a detector network depends on GW source strength, orientation of the binary axis and the geometrical configuration of the network (Wen & Chen 2010). Error ellipses of the order of tens to a few square degrees can be achieved through triangulation of time differences in signal arrival times at various detectors in a network (Gürsel & Tinto 1989; Fairhurst 2009).

The sensitivity distance, D_s , for sources uniformly distributed in orientation and sky location is approximated by $D_H/2.26$, where D_H is the horizon distance in Mpc at which an optimally orientated, overhead source can be detected with a signal-to-noise ratio of 8 (Abadie et al. 2010). We note that although D_H is based on the sensitivity of single detector, non-optimal effects such as non-Gaussian, non-stationary detector noise allow the approximation to be assumed for an Advanced LIGO/Virgo network (Abadie et al. 2010). Significantly, the value D_s of Advanced LIGO/Virgo for an NS–NS coalescence is smaller than the average distance to the observed SGRB population. This implies that EM emissions from NS–NS coalescences triggered by Advanced LIGO/Virgo will be brighter than the *Swift*-triggered⁸ GRB emissions. Nuttall & Sutton (2010) showed that a galaxy ranking procedure could identify the host galaxy 75–95 per cent of the time out to 100 Mpc for five images taken by narrow-field and wide-field telescopes, respectively. Their method depends on galaxy survey completeness, so may not be applicable for the Advanced GW detector network searches. We discuss the issues that will affect the localization of SGRBs in Section 4.

To estimate the optical flux of an SGRB as the EM counterpart of an NS–NS coalescence, we use the plausible estimates of Abadie et al. (2010) for the Advanced LIGO/Virgo sensitivity distances and detection rates of NS–NS coalescences. Taking a rate density of NS–NS coalescences $\sim 10^{-6} \text{ Mpc}^{-3} \text{ yr}^{-1}$ and $D_H = 445 \text{ Mpc}$, they find $D_s \approx 200 \text{ Mpc}$ and a detection rate $R_{\text{det}} \sim 40 \text{ yr}^{-1}$. This rate could potentially be increased by considering the improved signal-to-noise ratio for a coincident GW and optical search. The estimated increase in signal-to-noise ratio is about 1.5, assuming a narrow coincidence window, but the optical afterglows may not be imaged until hours after the GW trigger. None the less, the afterglows should be relatively bright at the distances we are considering, so it is possible that light curves could be extracted and extrapolated to earlier times. Hence, we assume that the sensitivity distance increases by a factor of 1.5, to 300 Mpc, so that $R_{\text{det}} \sim 135 \text{ yr}^{-1}$.

In this Letter we investigate the temporally varying optical brightness of SGRBs at the Advanced LIGO/Virgo sensitivity distance to NS–NS coalescences, from the first hour of the EM emission to about 100 d later. We use optical data for three SGRBs, GRB 050724, GRB 050709 and GRB 051221, that show evidence for collimated emission and are localized. Assuming that all NS–NS mergers produce jets, we use these data combined with reasonable estimates of the NS–NS coalescence rate detected by a GW detector

² <http://www.ligo.caltech.edu/>

³ <http://www.virgo.infn.it/>

⁴ <http://www.geo600.uni-hannover.de>

⁵ <http://www.ligo.caltech.edu/advLIGO/>

⁶ <http://www.ego-gw.it/public/virgo/virgo.aspx>

⁷ In practice, for sources not associated with host galaxies, the inclination angle has a strong degeneracy with distance, particularly for angles less than 45° .

⁸ <http://swift.gsfc.nasa.gov/docs/swift/swiftsc.html>

network to determine the fraction of events that could be potentially detected as both on- and off-axis bursts. For definiteness, we use the sensitivity limits of two robotic telescopes, TAROT ($m = 18$, see Klotz et al. 2008) and Zadko ($m = 21$, see Coward et al. 2010), that have participated in the optical follow-up of LIGO/Virgo GW triggers as part of the LOOC UP programme during the 6th Science Run (Kanner et al. 2008). We also include a much deeper sensitivity limit of $m = 26$, representative of an 8–10 m class telescope such as the VLT.⁹ Finally, we discuss the main issues that need addressing to interpret and optimize the science return from joint optical and GW searches.

2 OPTICAL AFTERGLOW MODEL AND COINCIDENT RATES

2.1 Observations

In order to constrain the detection rate, we require localization (including redshift), beaming angles and the optical flux values for our sample of bursts. We use three SGRBs that have estimates for these parameters, namely GRB 050709, GRB 050724 and GRB 051221A.

GRB 050709. From comparison of X-ray and optical data, a jet-break is present in the optical at about 10 d after the burst (Fox et al. 2005). On the other hand, Watson et al. (2006) claimed that the light curves were not displaying such a break. We note, however, that they excluded one optical data point within their fit, arguing it was coincident with a late X-ray flare. However, the data point they excluded was 9.8 d after the burst, compared to 16 d for the X-ray flare. We assume the explanation of Fox et al. (2005), noting that the detection of the jet-break is supported by only one data point.

GRB 050724. From radio and near-infrared data, Panaitescu (2006) and Berger et al. (2005) claimed evidence of a jet-break about 1 d after the burst. However, the main feature of the jet-break is its achromaticity (Rhoads 1999), and the X-ray data do not feature such a break (Gruppe et al. 2006). The X-ray light curve is consistent with no jet-break up to 22 d after the event, or $\theta_j > 25^\circ$.

GRB 051221A. The detection of the jet-break was observed in X-ray only (Soderberg et al. 2006). A jet-break is clearly visible in the light curve at about 5 d post-burst.

We note that determination of the jet opening angle from the break time is strongly sensitive on the model parameters used. In the previous cases, the model was always the same (a forward shock fireball expanding with kinetic energy E in a medium of constant density n), where $\theta \propto (n/E)^{1/8}$. However, n and E are uncertain in all bursts (see e.g. Panaitescu 2006 for the values of n in the cases of GRB 050709 and GRB 050724). Hence, opening angle values reported in these papers are taken as indicative values, and we use them as a guide (this is why we do not perform a k -correction for cosmological effects, as the correction is small compared to the uncertainties of the beaming angles).

2.2 Afterglow model and rates

For GRB 050724, GRB 050709 and GRB 051221, we define F_{11h} using R -band fluxes at 11 h from Nysewander, Fruchter & Pe'er

Table 1. The main observed and derived parameters of GRB 050724, GRB 050709 and GRB 051221. See Section 2.1 for caveats and uncertainties in θ_j .

GRB	$\log E_{\text{iso}}$	z	R mag (1 h) ^a	t_j (d)	θ_j ($^\circ$)
050724	50.21	0.26	12.7	<22	25
050709	49.06	0.16	17.2	10	14
051221	50.95	0.55	13.7	5	7

^aMagnitudes are converted from flux (Jy) to the AB magnitude system using $m_{\text{AB}} = -2.5 \log(F) + 8.9$ at a source distance of 300 Mpc.

(2009), but scaled to a source distance of 300 Mpc (the mean sensitivity distance of the GW search). Equation (1) scales the flux using a power-law index α_1 until jet-break time $t \leq t_{j,0}$, when the beamed emission starts to expand sideways, and by the luminosity distance to the source $d_L(z)$:

$$F(t, z) = \left(\frac{t}{11 \text{ h}} \right)^{\alpha_1} F_{11h} \left[\frac{d_L(z)}{D_s} \right]^2. \quad (1)$$

The above equation can be used to estimate the R -band flux at times before the jet-break. To model the SGRB light curve at post-jet-break times, we employ a smoothly joined broken power law (Beuermann et al. 1999),

$$F(t) = F_j \left[\left(\frac{t}{t_j} \right)^{-\alpha_1 n} + \left(\frac{t}{t_j} \right)^{-\alpha_2 n} \right]^{-1/n}, \quad (2)$$

where F_j is the flux at the jet-break time t_j , α_1 and α_2 are the pre-break and post-break light-curve slopes and n scales the sharpness of the break. The beaming angles and break times for GRB 050724, GRB 050709 and GRB 051221 are (25° , 22 d), (14° , 10 d) and (7° , 5 d), respectively, with corresponding power-law indices of α_1 and α_2 (-1.5 , -2), (-1.25 , -2.83) and (-1 , -2).

Table 1 shows the derived parameters with the extrapolated R -band magnitude at 1 h post-burst at 300 Mpc. We point out that the optical data used in the references to derive the beaming angle and break times are uncertain, and we do not account for optical bumps and flares that can be significant, especially at early times. None the less, it is clear from Table 1 that if one of the well-localized SGRBs occurred within D_s , and was on-axis, it would be bright at early times and easily detected by modest aperture telescopes.

Calculating the rate of triggered detection of on-axis afterglows requires accounting for the beaming angle θ_j . Equation (3) calculates the number of afterglows seen per year for a certain θ_j assuming a LIGO/Virgo detection rate of $R_{\text{det}} \sim 135 \text{ yr}^{-1}$ (see Section 1.1):

$$R_{\text{on}} = R_{\text{det}} [1 - \cos(\theta_j)]. \quad (3)$$

The rate of off-axis bursts is determined by the maximum angle, θ_{max} , away from the jet centre that an off-axis observer could see the afterglow. This angle depends critically on the flux limit of the telescope F_{lim} , F_j and θ_j . For off-axis detection, the main constraint is that the off-axis emission only becomes visible after the jet-break time, which may be days after the prompt burst. Totani & Panaitescu (2002), assuming the uniform jet model, show that θ_{max} can be expressed as

$$\theta_{\text{max}} = \left[2^{-(3+\delta)} \frac{F_j}{F_{\text{lim}}} \right]^{-1/(2\alpha_2)} \theta_j, \quad (4)$$

where α_2 is the post-break optical decay index and δ is a numerical factor ~ 1 . θ_j can be replaced with θ_{max} in equation (4) to estimate the SGRB off-axis detection rate:

$$R_{\text{off}}(\theta_{\text{max}}) = R_{\text{det}} [1 - \cos(\theta_{\text{max}})] - R_{\text{on}}. \quad (5)$$

⁹The Very Large Telescope, see <http://www.eso.org/public/teles-instr/vlt.html>

We note that if $\theta_{\max} \leq \theta_j$ only on-axis afterglows will be visible at any time, and the rate is determined by θ_j .

3 RESULTS

Using the above relations and light-curve characteristics for GRB 050724, GRB 050709 and GRB 051221, we extrapolate the light curves beyond the jet-break times to constrain detection limits, rates and cadence times using the sensitivities of TAROT, Zadko and an 8–10 m class telescope. Fig. 1 shows the temporal evolution of the three R-band light curves using equations (1) and (2) at a source distance of 300 Mpc, and published values for the decay indices. The three curves are quite different; GRB 050724 and GRB 051221 are relatively bright at early times, and can be seen from days to some tens of days by metre class telescopes.

Table 2 shows θ_{\max} , the detection rates R_{on} and R_{off} , and the maximum possible times that an on-axis burst would be visible for the three telescopes. We find that GRB 050724 like bursts are detectable at a relatively high rate. This is because the initial beaming angle is large ($>25^\circ$), so more of the afterglows can be seen on-axis. Conversely, the brightest afterglow at the post-break time, GRB 051221, is the least likely to be detected because of the small $\theta_j \sim 7^\circ$. It is apparent that both TAROT and Zadko are unlikely to detect off-axis afterglows from these SGRBs, but a telescope capable of deep imaging to $m = 26$ could detect an additional five afterglows per year for GRB 051221 like events.

Table 2 also shows the maximum time, t_{\max} , that the telescopes could detect the SGRB afterglows. This sets the limit on the cadence times for imaging. GRB 051221 has the brightest afterglow and is potentially detectable the longest time, $t_{\max} \sim 11$ d for Zadko. Given that the GW error ellipse is of the order of degrees in size, identification of a transient is more feasible for this afterglow type. Unfortunately, they occur at a rate of 1 yr^{-1} , and given optical selection effects (see Section 4 for a discussion) may be missed altogether. GRB 050724 like events, occurring at an optimistic rate of 13 yr^{-1} , would be detectable up to 5 d by Zadko. This would

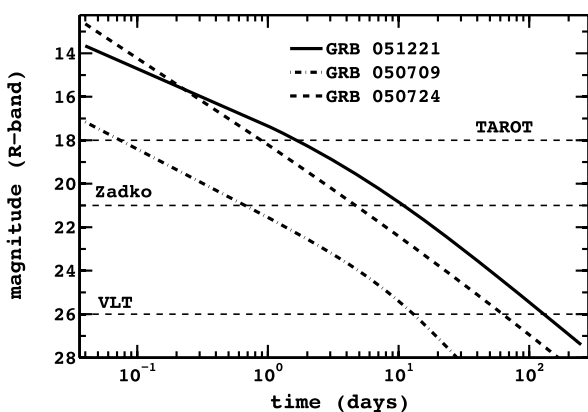


Figure 1. Three model light curves using equation (2) for GRB 050724, GRB 050709 and GRB 051221 extrapolated to a source distance of 300 Mpc, the horizon limit for the Advanced LIGO/Virgo detector network. The beaming angles and break times for the model bursts are (25° , 22 d), (14° , 10 d) and (7° , 5 d), respectively. Power-law indices before and after the breaks are $(-1.5, -2)$, $(-1.25, -2.83)$ and $(-1, -2)$, respectively. The horizontal dashed lines from bottom to top are the approximate sensitivities for an 8–10 m class telescope, Zadko Telescope (1 m) and TAROT (0.25 m), respectively. The maximum on-axis times for visibility are shown in Table 2.

Table 2. Equation (4) is used to calculate the maximum off-axis angle that the three SGRBs could be observed assuming limiting magnitudes of TAROT, Zadko and an 8–10 m class telescope such as VLT. Equations (3) and (5) are used to calculate both on- and off-axis rates of SGRB afterglows associated with GW emission from NS–NS coalescences detected by a three-detector network of GW detectors. The maximum time, t_{\max} , for detecting the optical afterglows for the three telescope sensitivities is also shown. The median and most optimistic on-axis detection rates are 4 and 13 yr^{-1} , respectively.

GRB	Telescope	θ_{\max} ($^\circ$)	R_{on} (yr^{-1})	R_{off} (yr^{-1})	t_{\max} (d)
050724	TAROT	$\theta_{\max} < \theta_j$	13	0	1
	Zadko	–	13	0	5
	VLT	$\theta_{\max} \sim \theta_j$	13	0	60
050709	TAROT	$\theta_{\max} < \theta_j$	4	0	0.08
	Zadko	–	4	0	1
	VLT	–	4	0	13
051221	TAROT	$\theta_{\max} < \theta_j$	1	0	2
	Zadko	–	1	0	11
	VLT	18	1	5	130

The maximum off-axis viewing angle, θ_{\max} , is not shown for afterglows with $\theta_{\max} < \theta_j$. This also implies a non-detection of an off-axis afterglow. The rates are upper limits and do not account for Galactic extinction and crowded fields.

allow time for surveying degree-size fields and multiple telescopes at different longitudes to perform follow-up imaging.

Our results in Table 2, based on a broad distribution of beaming angles, suggest that the optimal strategy for identifying the optical emissions triggered by GW detectors is through initial rapid response searches with robotic telescopes, followed by deeper imaging at later times if an afterglow is not detected within several days of the trigger.

4 DISCUSSION

The first attempts for a triggered search of the optical counterparts of NS–NS coalescences using GW detectors are just commencing. There are many uncertainties and issues that will need careful consideration for these types of searches. First, our results show that the coincident detection rate depends critically on the beaming angle distribution. For nearly isotropic optical emission, similar to GRB 050724, the coincident rates are very promising and will improve the confidence of the GW detection and provide much-needed localization. Even non-detections of optical emissions for high signal-to-noise ratio NS–NS GW candidates are interesting. Non-detections of a statistically significant sample would constrain the SGRB beaming angle distribution, or show that SGRBs are not linked to NS–NS coalescences. Both implications are critical to our understanding of the progenitors of SGRBs.

Full use of joint optical and GW observations requires understanding and accounting for selection effects that have historically plagued SGRB optical observations. Typical selection effects include Galactic extinction and crowded star fields. There is also the problem of host galaxy extinction, although this is expected to be a less of a problem given that at least some of the afterglows are observed off-set from the hosts. From the current optical follow-up attempts of *Swift*-triggered bursts, it is clear that a significant fraction of SGRBs that are apparently on-axis have not been observed in the optical at all. This can partly be attributed to the

much greater distances of the *Swift* bursts, compared to a GW-triggered search. We have based our calculations on a sensitivity distance of ~ 200 Mpc (non-coincidence rate), but note that GW wave sources with smaller angles of inclination will be detected at greater distances. Preliminary studies suggest that this bias can increase the median distance to ~ 269 Mpc for binaries with inclination angles less than 25° . A numerical study is planned to investigate how this bias will affect the rate of coincident detections.

Another important issue for the joint searches is the large errors in the GW source localization, which can extend to some tens of degrees. This is a significant problem given that the first observed GRB optical afterglows required small error boxes of arcmin size. To counter this, the GW-triggered search strategy will use the estimated horizon distance of the detector network to reduce the number of potential host galaxies, as opposed to a ‘blind’ error box that extends to cosmological distances. This technique was demonstrated in the recent LIGO/Virgo S6; the telescope pointing strategy used a galaxy weighting taking into account the mass and the distance of catalogued galaxies. A detailed description and analysis of the S6 coincidence searches will be published as a LIGO Scientific Collaboration paper.

Another problem that manifests with large coincidence error boxes is the increasing chance of detecting false coincident optical transients. False coincident sources may include supernovae, flare stars, variable active galactic nuclei and even Earth orbiting space debris. Fortunately, some of these sources can be excluded in the analysis because of the sensitivity distance of GW searches and the expectation that the strongest GW sources will be associated with catalogued host galaxies. Another possibility for optimizing the coincidence search is to data mine archived images from very wide field optical surveys, such as SkyMapper,¹⁰ and into the future the planned Large Synoptic Survey Telescope.¹¹

Given the above practical difficulties, an observed association of an optical transient with an NS–NS coalescence triggered by Advanced LIGO/Virgo is challenging. But, the science pay-off for such a discovery is enormous and provides motivation to address the issues discussed here in more detail. Now is the time to determine the optimal strategies for optical follow-up in readiness for the more sensitive GW searches in the following years. To accomplish this,

we will require a more comprehensive understanding of optical selection effects, the false alarm rate expected from SGRBs within the error ellipses of GW networks, and techniques to improve the localization of the host galaxy.

ACKNOWLEDGMENTS

DMC is supported by an Australian Research Council Future Fellowship. PJS was supported in part by STFC grant 500704.

REFERENCES

- Abadie J. et al., 2010, *Classical Quantum Gravity*, 27, 173001
 Acernese F. et al., 2009, *Advanced Virgo Baseline Design*, Virgo Internal Note, VIR-0027A-09
 Belczynski K. et al., 2006, *ApJ*, 648, 1110
 Berger E. et al., 2005, *Nat*, 438, 988
 Berger E. et al., 2007, *ApJ*, 664, 1000
 Beuermann K. et al., 1999, *A&A*, 352, L26
 Coward D. et al., 2010, *Publ. Astron. Soc. Australia*, 27, 331
 Eichler D. et al., 1989, *Nat*, 340, 126
 Fairhurst S., 2009, *New J. Phys.*, 11, 123006
 Fong W., Berger E., Fox D. B., 2010, *ApJ*, 708, 9
 Fox D. B. et al., 2005, *Nat*, 437, 845
 Gruppe et al., 2006, *ApJ*, 653, 462
 Gürsel Y., Tinto M., 1989, *Phys. Rev. D*, 40, 3884
 Harry G. M. et al., 2010, *Classical Quantum Gravity*, 27, 084006
 Kanner J. et al., 2008, *Classical Quantum Gravity*, 25, 184034
 Klotz A. et al., 2008, *PASP*, 120, 1298
 Klotz A. et al., 2009, *ApJ*, 697, L18
 Kochanek C. S., Piran T., 1993, *ApJ*, 417, L17
 Lee W. H., Ramirez-Ruiz E., Granot J., 2005, *ApJ*, 630, L165
 McWilliams S. T., Levin J., 2011, *Nat*, submitted (arXiv:1101.1969)
 Nakar E., 2007, *Phys. Rep.*, 442, 166
 Narayan R., Paczynski B., Piran T., 1992, *ApJ*, 395, L83
 Nuttall L., Sutton P., 2010, *Phys. Rev. D*, 82, 102002
 Nysewander M., Fruchter A. S., Pe’er A., 2009, *ApJ*, 701, 824
 Panaitescu A., 2006, *MNRAS*, 367, L42
 Rau A., Greiner J., Schwarz R., 2006, *A&A*, 449, 79
 Rhoads J. E., 1999, *ApJ*, 525, 737
 Soderberg A. M. et al., 2006, *ApJ*, 650, 261
 Totani T., Panaitescu A., 2002, *ApJ*, 576, 120
 Watson D. et al., 2006, *A&A*, 454, L123
 Wen L., Chen Y., 2010, *Phys. Rev. D*, 81, 082001
 Zheng Z., Ramirez-Ruiz E., 2007, *ApJ*, 665, 1220

¹⁰ <http://www.mso.anu.edu.au/skymapper/>

¹¹ <http://www.lsst.org/lsst>

This paper has been typeset from a $\text{\TeX}/\text{\LaTeX}$ file prepared by the author.